

## ON THE ROTATION PERIOD OF (90377) SEDNA

B. SCOTT GAUDI, KRZYSZTOF Z. STANEK, JOEL D. HARTMAN, MATTHEW J. HOLMAN, AND BRIAN A. MCLEOD

Harvard-Smithsonian Center for Astrophysics, 60 Garden Street, Cambridge, MA 02138; sgaudi@cfa.harvard.edu

Received 2005 March 30; accepted 2005 June 28; published 2005 July 21

### ABSTRACT

We present precise,  $\sim 1\%$ ,  $r$ -band relative photometry of the unusual solar system object (90377) Sedna. Our data consist of 143 data points taken over eight nights in 2004 October and 2005 January 2005. The rms variability over the longest contiguous stretch of five nights of data spanning 9 days is only  $\sim 1.3\%$ . This subset of data alone constrains the amplitude of any long-period variations with period  $P$  to be  $A \lesssim 1\%(P/20 \text{ days})^2$ . Over the course of any given  $\sim 5$  hr segment, the data exhibit significant linear trends not seen in a comparison star of similar magnitude, and in a few cases these segments show clear evidence of curvature at the level of a few millimagnitudes per hour squared. These properties imply that the rotation period of Sedna is  $O(10 \text{ hr})$ ; it cannot be  $\leq 5$  hr nor can it be  $\geq 10$  days, unless the intrinsic light curve has significant and comparable power on multiple timescales, which is unlikely. A sinusoidal fit yields a period of  $P = 10.273 \pm 0.002$  hr and a semiamplitude of  $A = 1.1\% \pm 0.1\%$ . There are additional acceptable fits with flanking periods separated by  $\sim 3$  minutes as well as another class of fits with  $P \sim 18$  hr, although these later fits appear less viable based on visual inspection. Our results indicate that the period of Sedna is likely consistent with typical rotation periods of solar system objects, thus obviating the need for a massive companion to slow its rotation.

*Subject headings:* Kuiper Belt — minor planets, asteroids — Oort Cloud — solar system: general

*Online material:* color figures, machine-readable table

### 1. INTRODUCTION

There is increasing evidence for the existence of an extended scattered disk: a massive population of objects orbiting beyond the Kuiper Belt (Gladman et al. 2002). These objects have orbits with substantial eccentricities and inclinations and are distinct from Kuiper Belt objects (KBOs) in that their perihelia are little affected by gravitational perturbations from Neptune. Thus, it appears that Neptune cannot be responsible for their unusual orbits, and several novel mechanisms to explain the origin of these objects have been proposed (Morbidelli & Levison 2004; Kenyon & Bromley 2004; Stern 2005). The total mass in these objects is poorly known because only a handful of members have been discovered. These include the recently detected object (90377) Sedna (= 2003 VB<sub>12</sub>), whose orbit has a semimajor axis of  $a \approx 500$  AU and a perihelion of  $q \approx 80$  AU (Brown et al. 2004a).

Sedna appears to be extreme in several ways in addition to its unusual orbit. It is intrinsically bright, with an absolute magnitude of  $H = 1.6$ , implying that it is one of the largest known minor planets. Unpublished reports also indicate that it is quite red, has a relatively high albedo, a weak opposition surge, and has a very long rotation period, with  $P \sim 20$ – $40$  days (Brown et al. 2004b). The latter claim is especially interesting in light of the fact that a *Hubble Space Telescope* snapshot of Sedna revealed no evidence of a large companion that could have tidally decreased Sedna's rotation period from typical solar system rotation periods of  $O(10 \text{ hr})$  to a longer period of  $\sim 20$  days.

Here we present precise relative photometry of Sedna that indicates a rotation period of  $O(10 \text{ hr})$  and rules out rotation periods longer than  $\sim 10$  days, under reasonable assumptions. The rotation period of Sedna is likely within the range of typical solar system objects, obviating the need for a massive companion.

### 2. OBSERVATIONS AND DATA REDUCTION

We observed Sedna over eight nights in 2004 October (UT 2004 October 8, 9, and 16) and 2005 January (UT 2005 Jan

7–9, 11, and 15). Photometric data were obtained with the MegaCam CCD camera (McLeod et al. 2000) on the MMT 6.5 m telescope. The MegaCam instrument uses  $36 \times 2048 \times 4608$  CCDs to cover a  $24' \times 24'$  field of view with a pixel scale of  $0''.08$ . Our primary science goal was to search for small KBOs, but we chose to target the field of Sedna to simultaneously acquire a precise light curve for this unusual object. The results of the KBO search will be presented elsewhere. Conditions during the observations ranged from good to poor, with image FWHMs in the range  $0''.7$ – $1''.9$ . All data were taken with a Sloan  $r$ -band filter with  $2 \times 2$  image binning. Exposure times were 300–450 s. The apparent motion of Sedna during our observations was  $\sim 1'' \text{ hr}^{-1}$ , so trailing losses are negligible.

The images were further binned and then reduced in the usual manner. Photometry was performed in two ways: using PSF-fitting photometry with the DAOPHOT II package (Stetson 1987, 1992) and image-subtraction photometry with the ISIS 2.1 package (Alard & Lupton 1998; Alard 2000). For the DAOPHOT reductions, relative photometry of Sedna was derived using 10–50 reference stars.

For moving objects, one must take care to consider background stars or galaxies that may be blended with the target in only a subset of exposures, potentially leading to artificial variability when using PSF-fitting photometry. In fact, during the night of UT 2004 January 8, Sedna was blended with a background object that was  $\sim 3.5$  mag fainter. Image-subtraction photometry eliminates any constant, stationary objects and so removes such contamination. On the other hand, the quality of PSF-fitting photometry can be comparable to image-subtraction photometry for uncontaminated objects in relatively sparse fields. Furthermore, we have found that DAOPHOT can extract reliable measurements from very poor quality frames, where ISIS fails. Therefore, in order to provide the best possible photometry, we adopted a hybrid approach, combining PSF-fitting photometry for the nights that showed no evidence of contaminating background objects (UT 2004 October 8–9 and 16 and UT 2005 January 11) and image-subtraction photometry for

TABLE 1  
SEDNA RELATIVE PHOTOMETRY AND PHASE

Date	HJD - 2,45,0000	$\Delta r^a$	$\sigma_{\Delta r}$	Phase Angle (deg)
UT 2004 Oct 8 .....	3286.83028	-0.001	0.005	0.3759
	3286.84411	-0.004	0.006	0.3758
	3286.84823	-0.013	0.006	0.3757
	3286.85249	-0.001	0.007	0.3757
	3286.85723	-0.001	0.007	0.3757
	3286.86124	0.005	0.009	0.3757
3286.86525	-0.010	0.007	0.3756	

NOTE.—Table 1 is published in its entirety in the electronic edition of the *Astrophysical Journal*. A portion is shown here for guidance regarding its form and content.

<sup>a</sup> Note that the photometry has an arbitrary zero point that differs for the data taken during UT 2004 October 8–9, UT 2004 October 16, and UT 2005 January 7–15.

the remainder of the nights (UT 2005 January 7–9 and 15). We stress that, for nights with no contamination, the light curves produced by the two methods are completely consistent. We used the DAOPHOT-reported errors for all data, as we judged these to be more reliable than ISIS-reported errors.

Due to Sedna's proper motion, it was not possible to use the same reference stars or images and thus tie the photometry to the same zero point for the entire data set. Therefore, the data consist of three “chunks,” corresponding to data taken on UT 2004 October 8–9, UT 2004 October 16, and UT 2005 January 7–15. Each of these chunks has an independent zero point. Although the relative offset and absolute photometric calibration of these chunks could be determined by various methods, these methods all require additional data. These data are not currently available. We therefore chose to present only relative photometry. This final photometry, consisting of 143 data points, is listed in Table 1, where we have subtracted the error-weighted mean instrumental magnitude from each chunk. We note that the apparent magnitude of Sedna during our observations was approximately  $R \sim 21$ .

### 3. ANALYSIS

Figure 1 shows the light curve for Sedna, where each panel corresponds to a different night. The nights belonging to the three separate chunks are indicated; each chunk has an independent zero point. The solid curve is a sinusoidal model, which is described below.

Several relatively model-independent conclusions can be drawn from the properties of the light curve. First, the rms deviation during the largest chunk spanning nine nights during UT 2005 January 7–15 is only  $\sim 1.3\%$ . In addition, these data show no evidence of significant curvature; a simple second-order polynomial fit to the January data yields an upper limit to the coefficient of the quadratic term of  $c_2 \leq 440 \mu\text{mag day}^{-2}$ . This implies that if the light-curve amplitude is large, the rotation period must be long. For example, for a sinusoidal light curve, this corresponds a limit on the semi-amplitude of  $A \leq c_2 P^2 / 2\pi^2 \sim 1\% (P/20 \text{ days})^2$  for large  $P$ . Second, the data during any given individual night spanning  $\leq 5$  hr generally have very small rms deviations. For example, the rms for the night of UT 2004 October 8 is only 0.7%. Nevertheless, several nights show evidence of significant variability that is not seen in a comparison star of similar magnitude. In many cases, this variability is consistent with a simple linear trend, which argues that the period cannot be  $\leq 5$  hr. However, for a few nights, curvature is evident. For example, a second-order polynomial

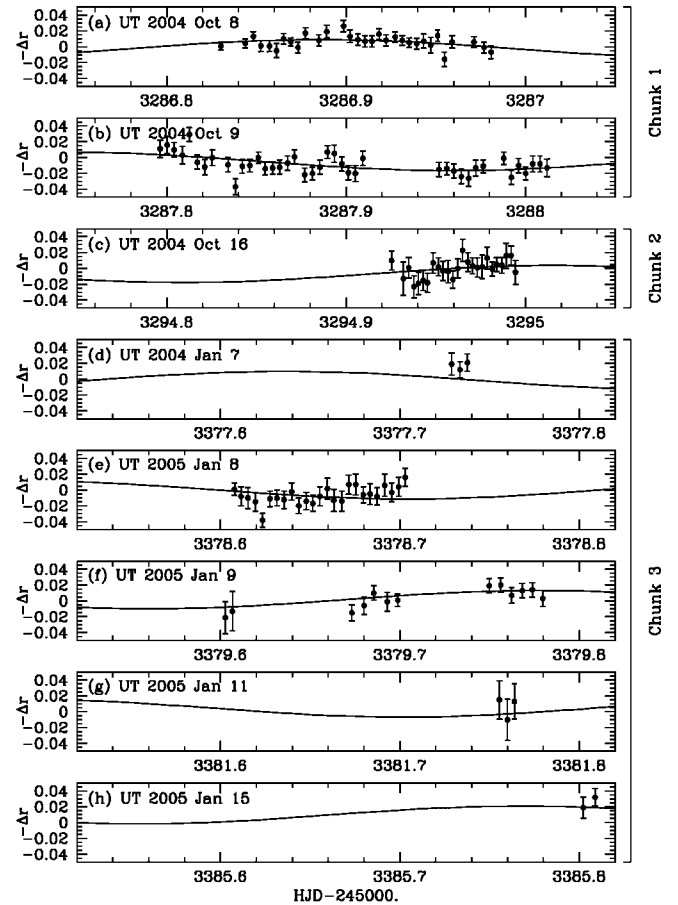


FIG. 1.—Relative photometry of Sedna. The data points show the  $r$  magnitude of Sedna vs. HJD - 2,450,000, relative to an arbitrary offset that is independent for each chunk. The solid line shows the best-fit sinusoidal model. Individual panels show data from the nights of (a) UT 2004 October 8, (b) UT 2004 October 9, (c) UT 2004 October 16, (d) UT 2005 January 7, (e) UT 2005 January 8, (f) UT 2005 January 9, (g) UT 2005 January 11, and (h) UT 2005 January 15.

fit to the UT 2004 October 8 data yields an  $\sim 3 \sigma$  detection of curvature with  $c_2 = -3.8 \pm 1.2 \text{ mmag hr}^{-2}$ . Similarly, a fit to the UT 2004 October 9 data yields  $c_2 = 2.0 \pm 0.9 \text{ mmag hr}^{-2}$ . The detection of significant curvature, the fact that the curvature on adjacent nights has opposite sign, and the fact that the difference in mean magnitudes between adjacent nights is  $\sim 1\%$  argue that the period must be  $O(10 \text{ hr})$ . This assumes that the primary power in the intrinsic light curve occurs at only one period. We believe this is a reasonable assumption.

We fit the light curve to the seven-parameter model,

$$F(t_i) = A \sin \left[ \frac{2\pi}{P} (t_i - t_0) + \phi_0 \right] - k[\alpha(t_i) - \alpha_0] + F_{0,j}, \quad (1)$$

where  $F(t_i)$  is the flux at the time  $t_i$  of observation  $i$ ,  $\alpha$  is the phase angle of Sedna at this time,  $k$  is the coefficient of the phase function,<sup>1</sup>  $F_{0,j}$  is the flux zero point for chunk  $j$ , and  $t_0 - 2,450,000 = 3308.23289$  and  $\alpha_0 = 0.4039$  are the error-weighted mean observation times and phase angles, respectively. Note that we are fitting relative photometry, and thus  $A$ ,  $k$ , and  $F_{0,j}$  are dimensionless. In practice, we expand the

<sup>1</sup> We have assumed a linear phase function. This is appropriate given the relatively small range of phase angles spanned by our data set (Bowell et al. 1989). See Table 1.

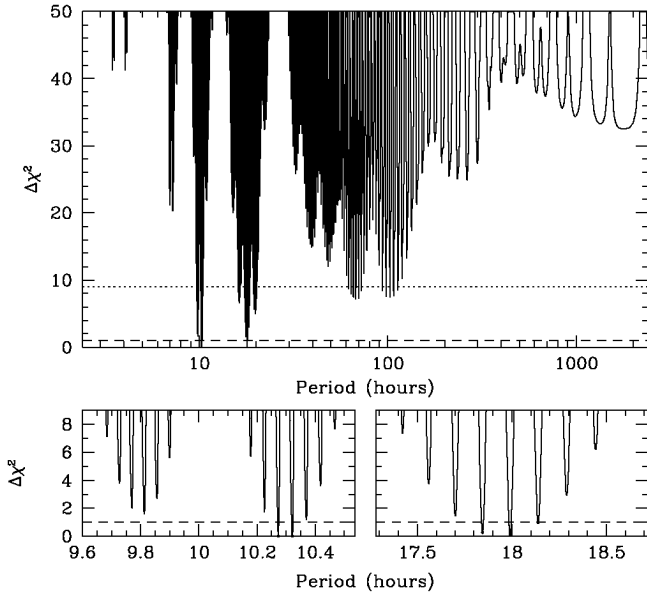


FIG. 2.—Difference in  $\chi^2$  of a sinusoidal model fit to the Sedna light curve from the minimum  $\chi^2$  of the best-fit model with  $P = 10.273 \pm 0.002$  hr, as a function of the period of the model. The top panel shows the full range of periods searched, whereas the bottom panels show close-ups of the two most significant classes of fits. The horizontal lines show  $\Delta\chi^2 = 1$  (dashed) and 9 (dotted). [See the electronic edition of the *Journal* for a color version of this figure.]

sinusoidal term in equation (1) into separate sine and cosine terms, and then perform a linear fit in flux to the coefficients of these terms, the phase angle term, and the constant terms. We then reconstruct the more physical parameters  $A$  and  $\phi_0$  from the coefficients of the sine and cosine terms. This has the advantages that the only nonlinear variable that must be fitted is  $P$  and that errors on the parameters  $A$ ,  $\phi_0$ ,  $k$ , and  $F_{0,j}$  can be determined analytically at fixed  $P$ . We constrain  $k$  to be within  $1 \sigma$  of the range  $0 \leq k \leq 0.3 \text{ deg}^{-1}$ , although the exact form of the constraint has little effect on the results. Note that, aside from the phase angle term, equation (1) is equivalent to a Lomb-Scargle periodogram with a floating mean (Lomb 1976; Scargle 1982; Cumming 2004).

We search for fits in the range  $-1 \leq \log(P/\text{day}) \leq 3$ , with steps of  $\delta P/P = 4 \times 10^{-6}$ . The resulting periodogram, here displayed as  $\Delta\chi^2 \equiv \chi^2 - \chi_{\min}^2$  versus  $P$ , is shown in Figure 2. The best fit has  $\chi_{\min}^2 = 150.0$  for  $143 - 7 = 136$  degrees of freedom (dof), indicating a good fit. For reference, a constant flux fit to the data yields  $\chi^2 = 272.4$  for 140 dof. Thus, the detection of variability, as judged by the improvement in  $\chi^2$ , is extremely significant. The parameters for the fit are  $P = 10.273 \pm 0.002$  hr and  $A = 1.1\% \pm 0.1\%$ . The phase angle coefficient  $k$  is poorly constrained, due to the fact that the separate chunks are not tied together, and thus the time baseline for determining  $k$  is limited to the  $\sim 9$  day span of our January

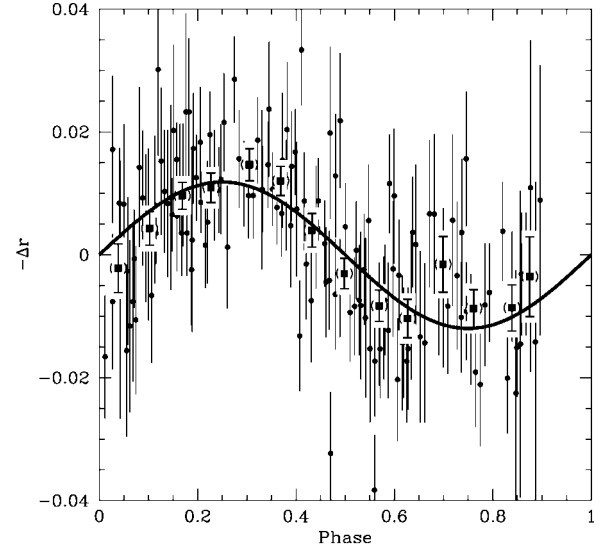


FIG. 3.—Black circles: Relative photometry of Sedna, phased to the best-fit period of  $P = 10.273 \pm 0.002$  hr, with the fitted zero point and phase variations subtracted. Black squares: Data binned into intervals of 0.067 in phase. The solid curve shows the best-fit sinusoidal model. [See the electronic edition of the *Journal* for a color version of this figure.]

data. Figure 3 shows the light curve phased to the best-fit period, with the constant flux and phase angle terms subtracted, along with the model fit. The model appears to describe the data reasonably well.

Flanking the best-fit period are additional fits separated by  $\sim 2.82$  minutes (see Fig. 2); these correspond to fits in which there are one or more additional cycles between the October and January data sets, i.e., where  $P_1^{-1} - P_2^{-1} \approx \pm n(90 \text{ days})^{-1}$  for integer  $n$ . In addition, there is a cluster of fits that is separated by  $\sim 27.6$  minutes from the best-fit period. These correspond to fits in which there is one additional cycle between UT October 9 and UT October 16. Finally, there are also diurnal aliases near  $P \approx 18$  hr and 3 days (and the associated aliases of these aliases). Fits near the latter period are allowed at the  $\sim 3 \sigma$  level.

We find a total of five fits that are statistically indistinguishable ( $\Delta\chi^2 \leq 1$ ) from the best fit. The parameters of these fits are given in Table 2. Two of these fits have  $P \sim 10$  hr, and appear equally good to the eye. The other three fits have  $P \approx 18$  hr. Although these fits are statistically acceptable, they appear much less convincing upon inspection of the phased light curves, one example of which is shown in Figure 4. The amplitude is relatively constant for all the acceptable fits, with  $A \approx 1\%$ . Models with  $P \geq 10$  days are ruled out at the  $>4 \sigma$  level. Refitting the data after subtracting the flux predicted by the best-fit model reveals no significant additional periodicities.

As a sanity check, we repeated the analysis described above on a light curve constructed from comparison stars of similar magnitude to Sedna. We find no evidence of variability at the

TABLE 2  
FIT PARAMETERS

$P$ (hr)	$A$	$\phi_0$	$k$ ( $\text{deg}^{-1}$ )	$F_{0,1}$	$F_{0,2}$	$F_{0,3}$	$\chi^2$ (136 dof)
$10.273 \pm 0.002$ .....	$0.011 \pm 0.001$	$0.73 \pm 0.12$	$0.2 \pm 0.2$	$1.004 \pm 0.001$	$1.015 \pm 0.002$	$0.970 \pm 0.002$	150.0
$10.321 \pm 0.002$ .....	$0.010 \pm 0.001$	$5.60 \pm 0.12$	$0.2 \pm 0.2$	$1.004 \pm 0.001$	$1.019 \pm 0.003$	$0.969 \pm 0.002$	150.0
$17.991 \pm 0.006$ .....	$0.011 \pm 0.002$	$4.43 \pm 0.17$	$0.2 \pm 0.2$	$1.001 \pm 0.008$	$1.016 \pm 0.025$	$0.978 \pm 0.036$	150.0
$17.845 \pm 0.006$ .....	$0.011 \pm 0.002$	$5.84 \pm 0.16$	$0.2 \pm 0.2$	$1.002 \pm 0.008$	$1.011 \pm 0.025$	$0.977 \pm 0.036$	150.2
$18.139 \pm 0.006$ .....	$0.010 \pm 0.002$	$3.01 \pm 0.18$	$0.2 \pm 0.2$	$1.003 \pm 0.008$	$1.026 \pm 0.025$	$0.971 \pm 0.036$	150.9

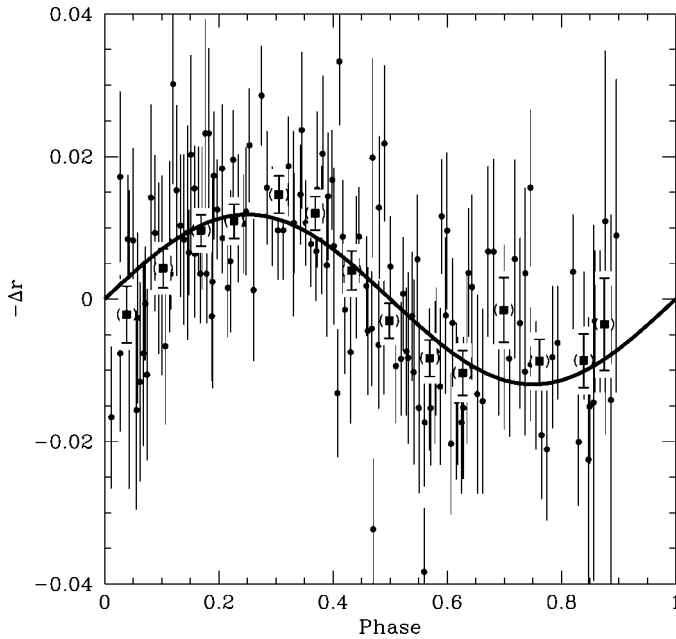


FIG. 4.—Same as Fig. 3, except for the best model of the second class of acceptable fits, with a period of  $P = 17.991 \pm 0.006$  hr. Although the  $\chi^2$  of this model for the unbinned data is nearly identical to that of the model with  $P = 10.273 \pm 0.002$  hr shown in Fig. 3, the  $\chi^2$  of the binned data is considerably worse. Thus, the model with  $P \sim 10$  hr is favored. [See the electronic edition of the *Journal* for a color version of this figure.]

level exhibited by Sedna. The best fit has an improvement in  $\chi^2$  over a constant flux model of  $\sim 38$  for 4 additional degrees of freedom, with an amplitude of only  $A = 0.38\% \pm 0.06\%$ .

#### 4. SUMMARY AND DISCUSSION

We have presented relative photometry of the unusual solar system object Sedna, obtained with the MMT 6.5 m telescope over eight nights in two campaigns in 2004 October and 2005 January. The light curve during the longest contiguous stretch of 9 days has a remarkably small rms of  $\sim 1.3\%$  and exhibits no significant curvature, which severely constrains the ampli-

tude of any long-term variability to  $A \leq 1\%(P/20 \text{ days})^2$ . The light curve during any individual night exhibits significant variability that is not seen in a comparison star of similar brightness. The photometry from several individual nights shows significant curvature over the span of  $\sim 5$  hr.

These properties indicate that the period of Sedna is  $O(10 \text{ hr})$  and cannot be larger than  $\sim 10$  days. A sinusoidal model fit to Sedna yields a best-fit period of  $P = 10.273 \pm 0.003$  hr and a semiamplitude  $A = 1.0\% \pm 0.1\%$ , with additional acceptable fits with flanking periods separated by  $\sim 3$  minutes as well as another class of fits with  $P \sim 18$  hr, although these later fits appear less viable based on visual inspection. We note that, if the variability is due to an aspherical shape such as a triaxial ellipsoid, the true rotation period is twice the fitted period. There also exist fits at the diurnal aliases of the primary period with  $P \sim 3$  days that are marginally acceptable at the  $3\sigma$  level. Fits with  $P \leq 10$  hr or  $P \geq 10$  days are ruled out at the  $\geq 3\sigma$  level. Thus, we conclude that the rotation period of Sedna is most likely  $P \sim 10$  hr, although other periods cannot be completely excluded. Additional observations should be pursued to distinguish between the various viable fits found here and to firmly identify the true rotation period of Sedna. The best-fit rotation period of  $\sim 10$  hr makes Sedna entirely typical of the bulk of solar system objects, including main-belt asteroids (Pravec & Harris 2000; Harris 2002) as well as the approximately dozen KBOs with measured rotation rates (Sheppard & Jewitt 2002).

We conclude that there is no real evidence that the period of Sedna is extraordinarily long ( $P \geq 10$  days) or even unusual. Therefore, there is no compelling reason to invoke a massive companion to spin down Sedna's rotation period.

B. S. G. was supported by a Menzel Fellowship from the Harvard College Observatory. K. Z. S. acknowledges support from the William F. Milton Fund. We would like to thank Roman Rafikov for helpful discussions, Scott Kenyon for reading the manuscript, and Perry Berlind, Emeric Le Floc'h, Casey Papovich, Jane Rigby, and Kurtis Williams for assistance in acquiring additional data.

#### REFERENCES

- Alard, C. 2000, *A&AS*, 144, 363  
 Alard, C., & Lupton, R. H. 1998, *ApJ*, 503, 325  
 Bowell, E., Hapke, B., Domingue, D., Lumme, K., Peltoniemi, J., & Harris, A. W. 1989, in *Asteroids II*, ed. R. P. Binzel, T. Gehrels, & M. S. Matthews (Tucson: Univ. Arizona Press), 524  
 Brown, M. E., Trujillo, C., & Rabinowitz, D. 2004a, *ApJ*, 617, 645  
 Brown, M. E., Trujillo, C. A., Rabinowitz, D., Stansberry, J., Bertoldi, F., & Koresko, C. D. 2004b, *DPS Meeting*, 36, 03.01  
 Cumming, A. 2004, *MNRAS*, 354, 1165  
 Gladman, B., Holman, M., Grav, T., Kavelaars, J., Nicholson, P., Aksnes, K., & Petit, J.-M. 2002, *Icarus*, 157, 269  
 Harris, A. W. 2002, *Icarus*, 156, 184  
 Kenyon, S. J., & Bromley, B. C. 2004, *Nature*, 432, 598  
 Lomb, N. R. 1976, *Ap&SS*, 39, 447  
 McLeod, B. A., Conroy, M., Gauron, T. M., Geary, J. C., & Ordway, M. P. 2000, in *Further Developments in Scientific Optical Imaging*, ed. M. Bonner Denton (Cambridge: R. Soc. Chem.), 11  
 Morbidelli, A., & Levison, H. F. 2004, *AJ*, 128, 2564  
 Pravec, P., & Harris, A. W. 2000, *Icarus*, 148, 12  
 Scargle, J. D. 1982, *ApJ*, 263, 835  
 Sheppard, S. S., & Jewitt, D. C. 2002, *AJ*, 124, 1757  
 Stern, S. A. 2005, *AJ*, 129, 526  
 Stetson, P. B. 1987, *PASP*, 99, 191  
 ———. 1992, in *ASP Conf. Ser. 25, Astrophysical Data Analysis Software and Systems I*, ed. D. M. Worrall, C. Bimesderfer, & J. Barnes (San Francisco: ASP), 297